



# Molecular characterization and expression analysis of the Na<sup>+</sup>/H<sup>+</sup> exchanger gene family in *Medicago truncatula*

Devinder Sandhu<sup>1</sup> · Manju V. Pudussery<sup>1</sup> · Rakesh Kaundal<sup>2</sup> · Donald L. Suarez<sup>1</sup> · Amita Kaundal<sup>1</sup> · Rajandeep S. Sekhon<sup>3</sup>

Received: 18 August 2017 / Revised: 4 December 2017 / Accepted: 8 December 2017 / Published online: 26 December 2017

© This is a U.S. government work and its text is not subject to copyright protection in the United States; however, its text may be subject to foreign copyright protection 2017

## Abstract

One important mechanism plants use to cope with salinity is keeping the cytosolic Na<sup>+</sup> concentration low by sequestering Na<sup>+</sup> in vacuoles, a process facilitated by Na<sup>+</sup>/H<sup>+</sup> exchangers (NHX). There are eight *NHX* genes (*NHX1* through *NHX8*) identified and characterized in *Arabidopsis thaliana*. Bioinformatics analyses of the known *Arabidopsis* genes enabled us to identify six *Medicago truncatula* NHX genes (*MtNHX1*, *MtNHX2*, *MtNHX3*, *MtNHX4*, *MtNHX6*, and *MtNHX7*). Twelve transmembrane domains and an amiloride binding site were conserved in five out of six MtNHX proteins. Phylogenetic analysis involving *A. thaliana*, *Glycine max*, *Phaseolus vulgaris*, and *M. truncatula* revealed that each individual MtNHX class (class I: MtNHX1 through 4; class II: MtNHX6; class III: MtNHX7) falls under a separate clade. In a salinity-stress experiment, *M. truncatula* exhibited ~20% reduction in biomass. In the salinity treatment, sodium contents increased by 178 and 75% in leaves and roots, respectively, and Cl<sup>-</sup> contents increased by 152 and 162%, respectively. Na<sup>+</sup> exclusion may be responsible for the relatively smaller increase in Na<sup>+</sup> concentration in roots under salt stress as compared to Cl<sup>-</sup>. Decline in tissue K<sup>+</sup> concentration under salinity was not surprising as some antiporters play an important role in transporting both Na<sup>+</sup> and K<sup>+</sup>. *MtNHX1*, *MtNHX6*, and *MtNHX7* display high expression in roots and leaves. *MtNHX3*, *MtNHX6*, and *MtNHX7* were induced in roots under salinity stress. Expression analysis results indicate that sequestering Na<sup>+</sup> into vacuoles may not be the principal component trait of the salt tolerance mechanism in *M. truncatula* and other component traits may be pivotal.

**Keywords** Salinity · *Medicago truncatula* · Salt tolerance · Na<sup>+</sup>/H<sup>+</sup> exchanger · NHX

## Introduction

Water is the most valuable and limiting resource for modern agriculture. Reduced availability of good-quality water is forcing farmers to use alternative or degraded waters, usually high

in salt concentration (Cooley et al. 2015). Salinity is a major abiotic stress with severe implications for the future of agriculture globally (Munns and Tester 2008). A significant and increasing proportion of the irrigated land worldwide is affected by salinity (Flowers and Yeo 1995).

**Electronic supplementary material** The online version of this article (<https://doi.org/10.1007/s10142-017-0581-9>) contains supplementary material, which is available to authorized users.

High concentrations of Na<sup>+</sup> in cytosol interfere with normal cellular processes and are toxic to cells. Plants develop several physiological and biochemical mechanisms to handle the increased salinity in soil or irrigation water. Two main mechanisms involved in regulating Na<sup>+</sup> concentration in cytosol are efflux of Na<sup>+</sup> from root to soil and Na<sup>+</sup> sequestration in the vacuoles (Cao et al. 2016). Plants that are tolerant to high salt concentrations develop efficient protein channels in the plasma membrane for excretion of Na<sup>+</sup> out of the roots and/or in vacuolar membrane to partition Na<sup>+</sup> into the vacuole (Gupta and Huang 2014; Munns and Tester 2008; Shi et al. 2002).

Studies conducted on net Na<sup>+</sup> fluxes into plant roots and net accumulation of Na<sup>+</sup> in symplast indicate that 70–95% of the Na<sup>+</sup> that goes into the root cells is excreted out (Tester and

✉ Devinder Sandhu  
devinder.sandhu@ars.usda.gov

<sup>1</sup> USDA-ARS US Salinity Lab, 450 W Big Springs Road, Riverside, CA 92507, USA

<sup>2</sup> Bioinformatics lab, Department of Plants, Soils, and Climate; Center for Integrated Biosystems, College of Agriculture and Applied Sciences, Utah State University, Logan, UT 84322, USA

<sup>3</sup> Department of Genetics and Biochemistry, Clemson University, Clemson, SC, USA



Davenport 2003). Efficient  $\text{Na}^+$  exclusion is known to be the key in providing salt tolerance in many plant species (Liu et al. 2015; Munns and Tester 2008). A salt overly sensitive (SOS) pathway plays an important role in excluding  $\text{Na}^+$  from plant roots (Qiu et al. 2002). SOS3, a calcium-triggered protein, when active, interacts with SOS2 to trigger its kinase activity. In turn, SOS2 phosphorylates NHX7/SOS1, a  $\text{Na}^+/\text{H}^+$  exchanger present in the plasma membrane, which pumps  $\text{Na}^+$  out of the roots (Shi et al. 2002). Upregulation of SOS1 was shown to be associated with salt tolerance in *Medicago* species (Liu et al. 2015; Sandhu et al. 2017). Although SOS1 plays a major role in  $\text{Na}^+$  efflux from the root, the low level of  $\text{Na}^+/\text{H}^+$  exchange activity observed in the *sos1* mutant suggests the involvement of some additional exchangers (Qiu et al. 2002).

Regardless of the efficient efflux mechanism to regulate  $\text{Na}^+$  concentration in root cells, the high rate of influx results in the accumulation of  $\text{Na}^+$  in the cytosol of root cells. Therefore, plants develop a second line of defense and keep the cytosolic concentration of  $\text{Na}^+$  low by compartmentalization of  $\text{Na}^+$  ions (Jiang et al. 2010). The common mechanism that manages  $\text{Na}^+$  concentrations in the cytosol by directing excess  $\text{Na}^+$  into the vacuole involves  $\text{Na}^+/\text{H}^+$  exchanger proteins (Gupta and Huang 2014; Munns and Tester 2008). The NHX family of  $\text{Na}^+/\text{H}^+$  exchangers uses the  $\text{H}^+$  gradient as a driving force and plays a key role in managing  $\text{Na}^+$  concentrations in plant tissues. In *Arabidopsis thaliana*, eight  $\text{Na}^+/\text{H}^+$  antiporters have been identified and characterized into three distinct classes (Sze et al. 2004). NHX1 through NHX4 are present in tonoplast (class I), NHX5 and NHX6 are specific to endosomal membranes {vesicles, Golgi, trans-Golgi network (TGN), and pre-vacuolar compartment (PVC)} (class II), and NHX7/SOS1 and NHX8 are located in the plasma membrane (class III) (Bassil and Blumwald 2014; Pardo et al. 2006). Of the plasma membrane NHX proteins, NHX7/SOS1 is a  $\text{Na}^+/\text{H}^+$  antiporter and NHX8 is a  $\text{Li}^+/\text{H}^+$  antiporter (An et al. 2007). The ubiquitousness of NHX proteins in higher eukaryotes and the conservation of each class of NHX proteins in a wide variety of organisms advocates for the uniqueness of cellular functions of vacuolar, endosomal, and plasma membrane NHXs. Plant NHXs regulate  $\text{Na}^+/\text{H}^+$  exchanges,  $\text{K}^+/\text{H}^+$  exchanges, and turgor pressure in the cell, thereby affecting salinity tolerance, K nutrition, and cell expansion/growth (Cao et al. 2016; Munns and Tester 2008).

Compartmentalization of  $\text{Na}^+$  in vacuoles is used by many plant species to keep cytosolic  $\text{Na}^+$  concentration levels low during salt stress (Cao et al. 2016; Munns and Tester 2008). A few genes have been isolated from various plant species that play an important role in sequestering  $\text{Na}^+$  into the vacuoles and keeping the  $\text{Na}^+$  content in cytosol low. Overexpression of *NHX1* has been shown to provide enhanced salt tolerance in several plant species such as *Arabidopsis* (Apse et al. 1999), tomato (Zhang and Blumwald 2001), wheat (Xue et al. 2004),

*Brassica* (Rajagopal et al. 2007), and mungbean (Mishra et al. 2014). Transformation of alfalfa using wheat *NHX2* (*TaNHX2*) led to enhanced salt tolerance due to intracellular potassium homeostasis (Zhang et al. 2015). The *Arabidopsis* double-knockout mutant, *nhx1nhx2*, had only 30% of the  $\text{K}^+$  concentration in vacuoles as compared to the wild-type plant, suggesting involvement of *NHX1* and *NHX2* in  $\text{K}^+/\text{H}^+$  exchange. *AtNHX1* mediates  $\text{Na}^+/\text{H}^+$  and  $\text{K}^+/\text{H}^+$  exchanges at similar rates, whereas *TaNHX2* exhibits a slight preference for  $\text{K}^+/\text{H}^+$  exchanges over  $\text{Na}^+/\text{H}^+$  exchanges. Transgenic plants maintained higher  $\text{K}^+$  content, perhaps due to low  $\text{K}^+$  efflux by decreasing the depolarization of the plasma membrane and high  $\text{K}^+$  absorption (Zhang et al. 2015). Transgenic plants expressing the *AtNHX3* gene complemented sensitivity to  $\text{K}^+$  deficiency phenotype in *nhx3* background and showed increased  $\text{K}^+/\text{H}^+$  rates relative to the wild types (Liu et al. 2010). On the other hand, knock-out mutant of *AtNHX4* resulted in low  $\text{Na}^+$  accumulation and enhanced tolerance for salt stress (Li et al. 2009).

NHX5 and NHX6 co-localize with Golgi and trans-Golgi network (TGN) markers (Bassil et al. 2011a). Presumably, NHX5 and NHX6 affect trafficking from Golgi/TGN to vacuole, specifically of the proteins needed in response to high salt. Endosomal NHXs show strong preference for  $\text{K}^+/\text{H}^+$  exchanges over  $\text{Na}^+/\text{H}^+$  exchanges (Jiang et al. 2010). Presumably, endosomal/prevacuolar compartments in plants are sensitive to  $\text{Na}^+$  toxicity; hence, manipulation of endosomal NHXs for improved preference for  $\text{K}^+/\text{H}^+$  exchanges may prevent  $\text{Na}^+$  toxicity to endosomal compartments (Jiang et al. 2010). Silencing of *LeNHX2*, a PVC-located  $\text{Na}^+/\text{H}^+$  exchanger, resulted in increased sensitivity to  $\text{NaCl}$  in tomatoes (Rodríguez-Rosales et al. 2008).

Vacuoles maintain high amounts of  $\text{K}^+$  in the cell. In response to high  $\text{Na}^+$  concentration, cytosolic  $\text{Ca}^{2+}$  increases; this activates the SOS pathway. In addition to controlling efflux of  $\text{Na}^+$ , SOS2 also regulates vacuolar ATPase and vacuolar  $\text{Na}^+/\text{H}^+$  exchangers and plays an important role in compartmentalization of  $\text{Na}^+$  and  $\text{K}^+$  into the vacuole (Zhang et al. 2015). Increased sequestration of  $\text{K}^+$  into vacuoles leads to  $\text{K}^+$  deficiency in cytosol (Bassil et al. 2011b). Reduced  $\text{K}^+$  concentration in cytosol activates high affinity  $\text{K}^+$  uptake proteins located in the plasma membrane, which in turn leads to increased  $\text{K}^+$  uptake by plant roots.

Legumes are the world's most valuable crops with high levels of protein and oil; hence, they are important for human nutrition and for feed for livestock and aquaculture (Graham and Vance 2003). In addition to being major contributors to global crop production, legumes play an important role in symbiotic nitrogen fixation and save billions of dollars on nitrogen fertilizers (Graham and Vance 2003). The major legume crops include soybean, alfalfa, pea, chickpea, peanut, pigeon pea, lentils, and dry beans. *Medicago truncatula* is an ideal model legume that is an annual and diploid species with



a small genome size, a short life cycle, and a variety of genetic, genomic, and molecular tools (Tang et al. 2014). Characterization of  $\text{Na}^+/\text{H}^+$  exchangers in *M. truncatula* may be critical in understanding salt tolerance in legume crops and devising strategies for their management in high-salinity environments. In this investigation, we identified  $\text{Na}^+/\text{H}^+$  exchangers in *M. truncatula* and analyzed their structural and functional conservation. *M. truncatula* plants showed loss in biomass yield under salt stress and accumulated more  $\text{Na}^+$  and  $\text{Cl}^-$  in root and shoot tissues. An association of the expression patterns of the MtNHX genes with salt tolerance displayed some unique patterns as compared to the AtNHX genes highlighting some species-specific regulation of salt tolerance due to NHX proteins.

## Material and methods

### Sequence analyses of *M. truncatula* NHX genes

*Arabidopsis* NHX gene and protein sequences were used in Basic Local Alignment Search Tool (BLAST) analyses on the Phytozome website ([https://phytozome.jgi.doe.gov/pz/portal.html#!info?alias=Org\\_Mtruncatula](https://phytozome.jgi.doe.gov/pz/portal.html#!info?alias=Org_Mtruncatula)) to identify corresponding orthologs in *M. truncatula* (Supplementary Table 1). The full-length DNA and protein sequences were aligned using multiple sequence alignment program Clustal Omega (Sievers et al. 2011). The transmembrane domains were predicted using the TMHMM method (Krogh et al. 2001). Transmembrane domain structures of the MtNHX proteins were validated using information available for AtNHX proteins (Yokoi et al. 2002). Different protein sequences were aligned using the neighbor-joining method in the phylogenetic alignment program MEGA 6.0 (Saitou and Nei 1987; Tamura et al. 2013) using the MUSCLE alignment (Edgar 2004). The Poisson correction method was used to compute evolutionary distances that are represented as the number of amino acid substitutions per site (Zuckerandl and Pauling 1965).

### Plant material and salinity treatment

*M. truncatula* seeds were obtained from the USDA GRIN database. The *M. truncatula* line Jemalong A-17 (PI 670016) was used for the analyses. The experiment was conducted in the USDA ARS U.S. Salinity Laboratory greenhouse in Riverside, CA. Plants were grown in 0.66-gal pots, one plant per pot. The greenhouse conditions were as follows: daytime temperatures ranged between 23 and 27 °C and night temperatures between 12 and 15 °C; mid-day light intensity ranged from 700 to 900  $\mu\text{mol m}^{-2} \text{s}^{-1}$  with an average day length of 10 h and average relative humidity of 68%. The experimental setup consisted of a control and a salt treatment, each replicated four times. The plants were grown in a sandy

loam soil mix and were irrigated once a week either with tap water or with modified half Hoagland's solution (Fe 50  $\mu\text{mol L}^{-1}$  added as Fe-DTPA (Sprint 330®),  $\text{ZnSO}_4 \cdot 7\text{H}_2\text{O}$  1.2  $\mu\text{mol L}^{-1}$ ,  $\text{CuSO}_4 \cdot 5\text{H}_2\text{O}$  0.3  $\mu\text{mol L}^{-1}$ ,  $(\text{NH}_4)_6\text{Mo}_7\text{O}_{24} \cdot 4\text{H}_2\text{O}$  0.1  $\mu\text{mol L}^{-1}$ ,  $\text{H}_3\text{BO}_3$  23  $\mu\text{mol L}^{-1}$ , and  $\text{MnSO}_4$  15  $\mu\text{mol L}^{-1}$ ; and macronutrients:  $\text{KNO}_3$  5.0  $\text{mmol}_c \text{L}^{-1}$ ,  $\text{Ca}(\text{NO}_3)_2 \cdot 4\text{H}_2\text{O}$  0.5  $\text{mmol}_c \text{L}^{-1}$ ,  $\text{NaH}_2\text{PO}_4$  1.5  $\text{mmol}_c \text{L}^{-1}$ ,  $\text{CaCl}_2$  3.5  $\text{mmol}_c \text{L}^{-1}$ ,  $\text{CaSO}_4 \cdot 2\text{H}_2\text{O}$  1  $\text{mmol}_c \text{L}^{-1}$ ,  $\text{MgSO}_4 \cdot 7\text{H}_2\text{O}$  3.3  $\text{mmol}_c \text{L}^{-1}$ , and  $\text{Mg}(\text{NO}_3)_2 \cdot 6\text{H}_2\text{O}$  2.5  $\text{mmol}_c \text{L}^{-1}$ ) until the start of salt treatment. The composition of irrigation water is presented in Table 1.

Salt treatment was started 12 weeks after germination. To avoid osmotic shock or stress, the salinity level was increased in two steps. The treatment plants were irrigated with salt solution of electrical conductivity ( $\text{EC}_{\text{iw}}$ ) 5, 10, and 10  $\text{dS m}^{-1}$  in the first, second, and third week, respectively.  $\text{EC}_{\text{iw}}$  of the control and saline water treatment was measured with an electrical conductivity meter. The level of salinity (10  $\text{dS m}^{-1}$ ) was chosen based on our preliminary experiment on *M. truncatula* (data not shown). Weights of the pots containing plants were recorded before irrigation and after irrigation (once excess water was drained). The amount of water leached from each pot was also recorded. The control plants were irrigated with modified half Hoagland's solution ( $\text{EC} = 1.44 \text{ dS m}^{-1}$ ,  $\text{pH} = 6.77$ ) mentioned above.

### Ion composition

Plants were harvested 3 weeks after the initial salt treatment. Fresh root and shoot weights were recorded. Samples were washed with deionized water and quickly dried with paper towels. Root and shoot samples were used for the ion composition analysis. The samples were dried in a forced-air oven at 70 °C for 72 h and ground into a fine powder. The samples were digested with nitric acid in a microwave digester, and  $\text{Na}^+$ ,  $\text{K}^+$ ,  $\text{Mg}^{2+}$ ,  $\text{Ca}^{2+}$ , and micronutrients were determined using inductively coupled plasma optical emission spectrometry (ICP-OES) using ICP-OES Optima 8000 in three replicates following the manufacturer's recommendations (PerkinElmer Inc., Waltham, MA). Chlorides in the plant tissues were quantitatively extracted using water (Liu 1998) in two replicates and measured in a digital chloridometer (Chloride Titrator 4425000, Labconco, Kansas City, MO). Certified standards (SPEX) were used to make calibration curves for all the ions.

### Quantitative reverse transcription-PCR analyses

In the first experiment, we wanted to look at the expression of MtNHX genes in different plant tissues. For this experiment, we studied 4-month-old plants that started to produce flowers



**Table 1** Composition of the irrigation water

Treatment	EC <sub>iw</sub> (dS m <sup>-1</sup> )	pH	Ion concentration (mmol <sub>c</sub> L <sup>-1</sup> )							
			Cl <sup>-</sup>	SO <sub>4</sub> <sup>2-</sup>	NO <sub>3</sub> <sup>-</sup>	PO <sub>4</sub> <sup>3-</sup>	Na <sup>+</sup>	K <sup>+</sup>	Ca <sup>2+</sup>	Mg <sup>2+</sup>
Control	1.44	6.77	3.5	3	8	1.5	1.5	5	5	4.5
Saline	9.49	6.83	74	18	8	1.5	71.5	5	17	8

and fruits. Tissue samples were taken from roots, stems, leaves, flowers, and pods.

For the salinity experiment, young leaf and root samples were taken 48 h after initiating salt treatment (10 dS m<sup>-1</sup>) from 13-week-old plants. Previous studies and our preliminary work on salt tolerance in *M. truncatula* indicated that most useful expression responses are seen 48 h after salt treatment (Shavrukov 2013). RNA isolation was conducted using TRIzol® reagent (Invitrogen, Carlsbad, CA, USA). DNA contamination was removed by treating RNA samples with DNase I enzyme (Thermo Scientific, Waltham, MA, USA). Expression analysis was conducted using the reverse transcription-PCR (qRT-PCR) approach in a BioRad CFX96 System using iTaq™ Universal SYBR® Green One-Step Kit (Bio-Rad Laboratories, Hercules, CA, USA). Primers for different *M. truncatula* NHX genes were designed using the National Center of Biotechnology Information (NCBI) primer BLAST program (<https://www.ncbi.nlm.nih.gov/tools/>

primer-blast/). Based on the comparisons of the genomic DNA sequences and the coding DNA sequences (CDS), one PCR primer out of each pair was designed from two exons flanking an intron (Supplementary Table 2). The qRT-PCRs were carried out in a total volume of 10 µL that contained 100 ng RNA, 0.75 µM of each primer, 0.125 µL iScript™ Reverse Transcriptase enzyme, and 5 µL of 2× one-step SYBR® Green Reaction mix. The PCR program was as follows: 50 °C for 10 min, 95 °C for 1 min, then 40 cycles of 95 °C denaturation for 10 s, 57 °C annealing for 30 s, and 68 °C extension for 30 s. The *M. truncatula* genes *PDF2*, *PPRrep*, and *Ubiquitin* were used as reference genes. To calculate the normalized expression (ΔΔCq), the relative quantity of the target gene was normalized to the quantities of the reference genes (Vandesompele et al. 2002). The calculation of normalized expression is described by the following formula:

$$\text{normalized expression}_{\text{sample (GOI)}} = \left[ \text{RQ}_{\text{sample (GOI)}} \right] / \left[ \text{RQ}_{\text{sample (ref 1)}} \times \text{RQ}_{\text{sample (ref 2)}} \times \dots \times \text{RQ}_{\text{sample (ref n)}} \right]^{1/n}$$

where RQ is the relative quantity of a sample, ref is the reference target in a run that includes one or more reference targets in each sample, and GOI is gene of interest. The amplification specificity was tested using melt curve analysis using the program as follows: 95 °C for 10 s and back to 65 °C for 5 s followed by incremental increases of 0.5 °C/cycle up to 95 °C.

## Results

### Identification and structural analyses of *M. truncatula* NHX family genes

BLAST analysis of *Arabidopsis* NHX genes *AtNHX1* (AT5G27150), *AtNHX2* (AT3G05030), *AtNHX3* (AT5G55470), *AtNHX4* (AT3G06370), *AtNHX5* (AT1G54370), *AtNHX6* (AT1G79610), *AtNHX7* (AT2G01980), and *AtNHX8* (AT1G14660) resulted in the identification of eight genes in *M. truncatula*. To further support the orthologous relationship, the genomic DNA, CDS, and protein sequences were compared for all NHX sequences

in *Arabidopsis* and *M. truncatula* (Supplementary Table 1). AtNHX orthologs were identified for all *M. truncatula* NHX genes based on the protein homology (Supplementary Table 1). Exon-intron structure, domain structure, gene ontology (GO), and KEGG annotations were used to identify the corresponding genes in *Arabidopsis* and *M. truncatula* (Supplementary Table 1; Fig. 1; Supplementary Fig. 1). The identified *M. truncatula* NHX genes were named *MtNHX1–4*, *MtNHX6*, and *MtNHX7* and placed in three NHX classes (Table 2). MtNHX1 to MtNHX4 had between 71.2 and 76.6% identity at the amino acid level to their corresponding proteins in *A. thaliana* (Table 2; Supplementary Fig. 1). While MtNHX3 has the highest homology with AtNHX3, MtNHX1, MtNHX2, and MtNHX4 cannot be uniquely associated with any single AtNHX gene due to high sequence homology with more than one gene in their respective class (Table 2, Supplementary Table 2, Supplementary Fig. 1). There were no orthologous genes to *AtNHX5* or *AtNHX8* in *M. truncatula*; however, there were two additional homologs, *Medtr1g082440* and *Medtr1g082450*, which displayed 64 and 62% identity at amino acid level to AtNHX4, respectively

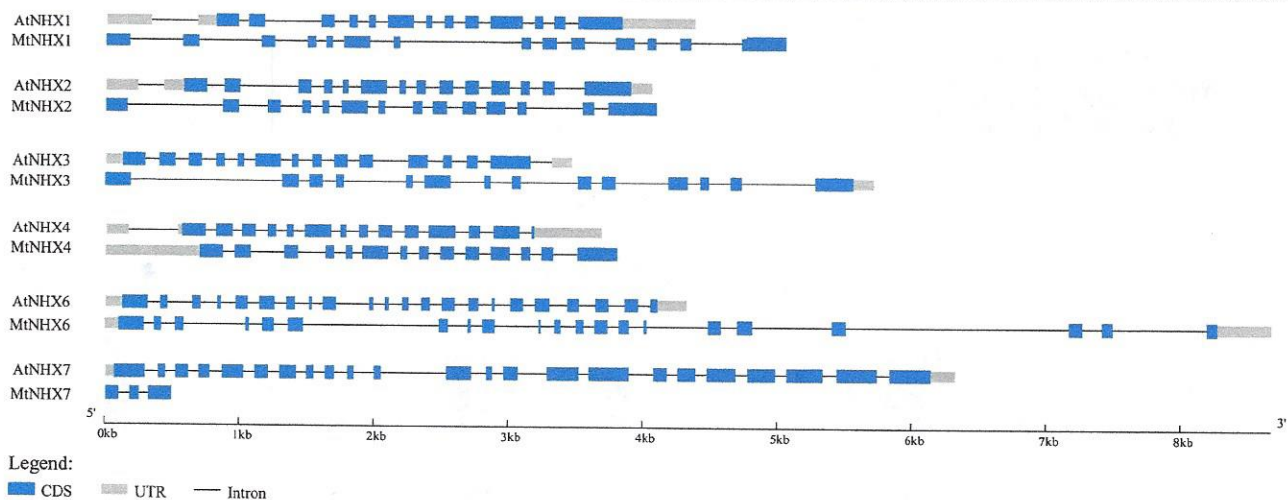


**Fig. 1** Structural organization of the MtNHX genes in comparison with the AtNHX genes. Exons are represented as rectangles; introns are represented as lines. Untranslated regions are represented as gray

rectangles, and translated regions are represented as blue rectangles. Structural organization was generated using Gene Structure Display Server 2.0 (Hu et al. 2015)

(Supplementary Fig. 1). *Medtr1g082440* and *Medtr1g082450* were present in tandem on chromosome 1 close to *MtNHX1* (Supplementary Fig. 2). *MtNHX2*, *MtNHX3*, *MtNHX4*, *MtNHX6*, and *MtNHX7* were located on chromosomes 7, 3, 4, 2, and 2, respectively (Supplementary Fig. 2).

The exon-intron structures of class II and class III genes were very different as compared to that of the class I genes (Table 2). *MtNHX1* to *MtNHX4* were similar in organization with 14 exons each and exon sizes were also well conserved (Fig. 1). At the genomic DNA level, *MtNHX6* was the largest gene with 21 exons and *MtNHX7* was the smallest with 3 exons (Table 2 and Fig. 1). At the protein sequence level, MtNXH7 was the smallest protein with a peptide length of 109 amino acids. Among the other five proteins (*MtNHX1*, *MtNHX2*, *MtNHX3*, *MtNHX4*, and *MtNHX6*), peptide length varied between 529 and 544 amino acids. Molecular weight deduced from the protein sequences for all other proteins, except *MtNHX7*, ranged between 58 and 60.35 kDa (Table 2). *MtNHX7* is

predicted to code for an 11.68-kDa protein. Isoelectric points of six proteins varied from 5.3 to 9.2 (Table 2).

### Conserved domain and phylogenetic analyses of *M. truncatula* NHX family genes

To study conservation among six *MtNHX* proteins, sequences were compared in similarity plots (Fig. 2). The analysis revealed that except for *MtNHX7*, 12 transmembrane (TM) domains and an amiloride binding site were conserved in five other *MtNHX* (*MtNHX1*, *MtNHX2*, *MtNHX3*, *MtNHX4*, *MtNHX6*) proteins (Fig. 2). Amiloride is a chemical that even in micromolar concentrations competitively inhibits Na<sup>+</sup> transport in Na<sup>+</sup>/H<sup>+</sup> exchangers in eukaryotes (Counillon et al. 1993). Many of the Na<sup>+</sup>/H<sup>+</sup> exchangers in animals and plants are known to have an amiloride binding site {(L/F)FF(I/L)(Y/F)LLPPI}. As previously shown in other plant NHX proteins, the amiloride binding site was present in TM3

**Table 2** NHX genes in *M. truncatula*

Gene name	Locus name	Genomic sequence	Transcript sequence	CDS sequence	Peptide sequence	Na <sup>+</sup> /H <sup>+</sup> exchanger domain (start to end)	NHX class	Subcellular localization prediction*	MW (kDa)	PI	% identity with the corresponding <i>Arabidopsis</i> NHX protein
<i>MtNHX1</i>	<i>Medtr1g081900</i>	5056	1626	1626	541	51–445	I	Vacuole	59.60	8	76.6*
<i>MtNHX2</i>	<i>Medtr7g114250</i>	4092	1635	1635	544	45–435	I	Vacuole	60.35	6	72.7*
<i>MtNHX3</i>	<i>Medtr3g055600</i>	5716	1753	1599	532	31–451	I	Vacuole	59.86	6	71.2
<i>MtNHX4</i>	<i>Medtr4g118770</i>	3801	2286	1590	529	50–444	I	Vacuole	58.83	9	73.7*
<i>MtNHX6</i>	<i>Medtr2g028230</i>	8675	2095	1593	530	111–428	II	Golgi	58.00	6	77.6*
<i>MtNHX7</i>	<i>Medtr2g038400</i>	488	330	330	109	30–106	III	Plasma membrane	11.68	5	64.6*

\*These *M. truncatula* genes share homology with multiple *Arabidopsis* NHX genes



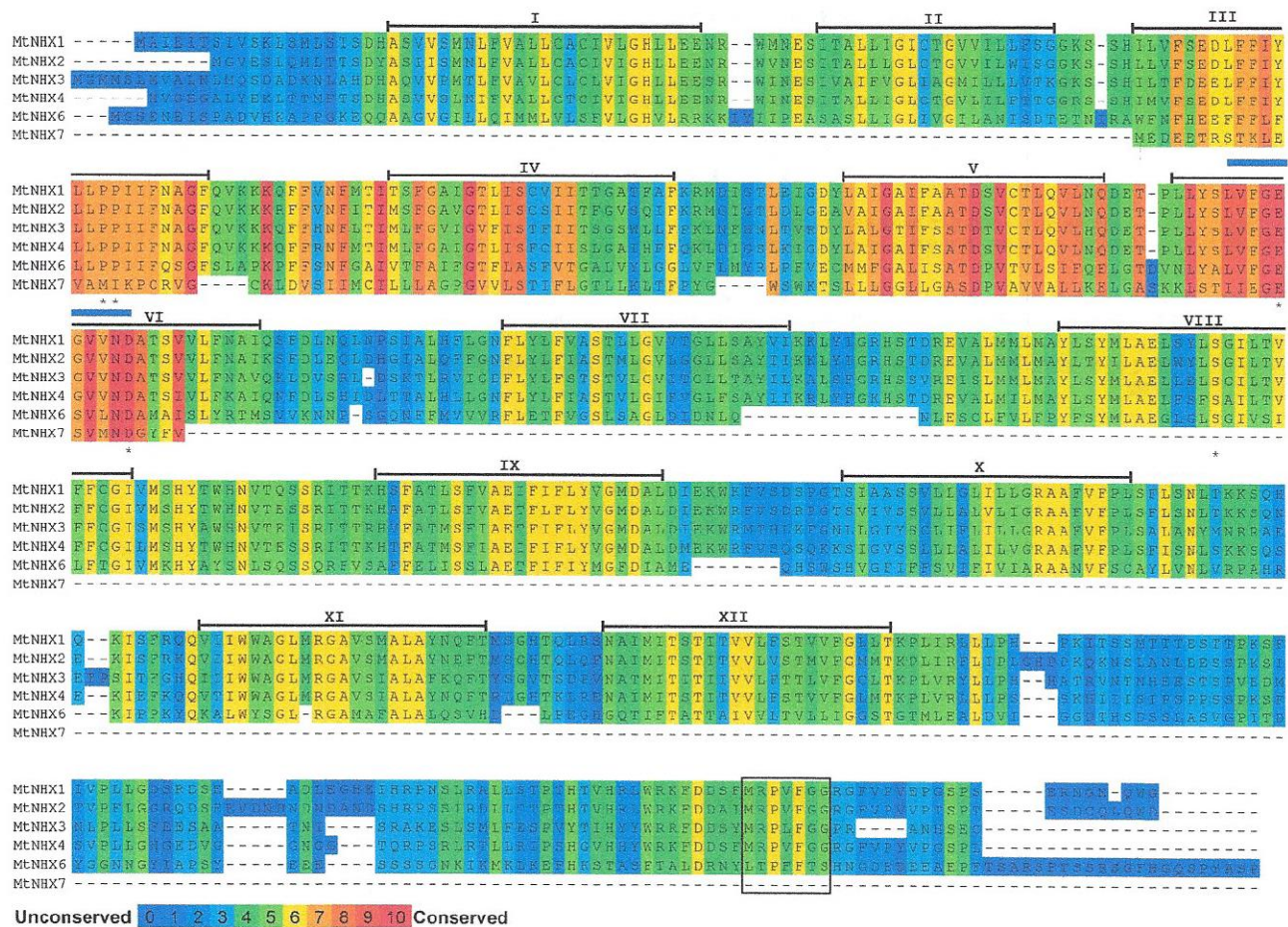


**Fig. 2** Multiple sequence alignment of the MtNHX proteins. Protein sequences were aligned using the Clustal Omega software. Putative transmembrane domains are represented by black lines over the sequences and labeled using Roman numerals. The amiloride binding

motif is represented by a blue line below the sequences. The residues important for antiport activity are marked with an asterisk below the sequences. The C-terminal region important for antiport activity is marked by a black box

(Fig. 2) (Cao et al. 2016). Additionally, two regions, one in TM5 and another one in TM6, were highly conserved among all six MtNHX proteins (Fig. 2). MtNHX1 to MtNHX4 were more closely associated with each other; on the other hand, MtNHX6 and MtNHX7 were more distantly related (Fig. 2).

Evolutionary relationships among the NHX gene family members were studied by computing an unrooted phylogram showing divergence in *A. thaliana*, *Glycine max*, *Phaseolus vulgaris*, and *M. truncatula* (Fig. 3). External nodes in the phylogram represent each protein sequence, and internal nodes display the percentage support for each divergence. Branch distances in the tree are shown in units of residue substitutions per site. The phylogenetic analysis revealed that each individual class in NHX falls under a separate clade. MtNHX1 through 4 (class I) were in one clade, MtNHX6 (class II) in another clade, and MtNHX7 (class III) in a separate clade (Fig. 3). AtNHX5 and AtNHX6 fell in the same clade as MtNHX6, and AtNHX7 and AtNHX8 fell in the same clade as MtNHX7 (Fig. 3). AtNHX1 and AtNHX2 were very similar; however, corresponding genes in *M. truncatula*, *P. vulgaris*, and *G. max* could

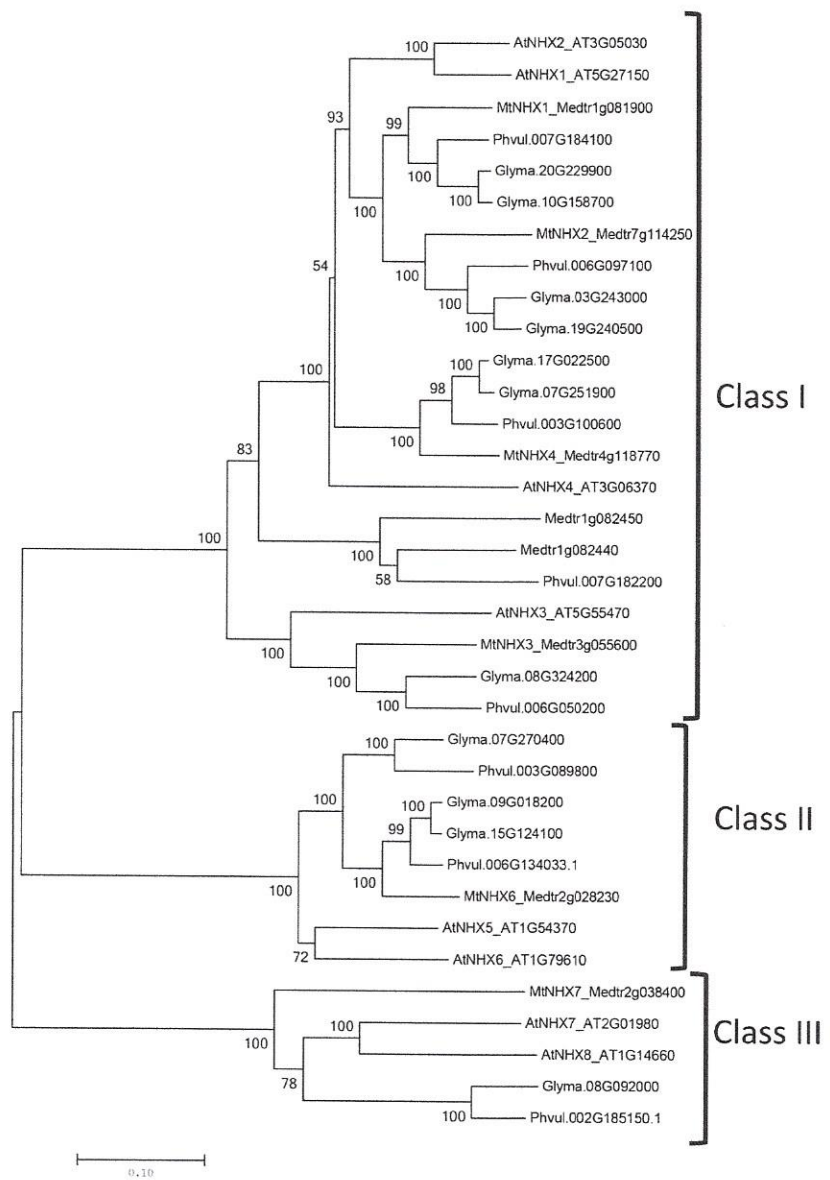
be separated into different groups (Fig. 3). Based on the evolutionary distance, MtNHX4 appeared to be more closely associated with MtNHX1 and MtNHX2. Two *M. truncatula* genes, *Medtr1g082440* and *Medtr1g082450*, which showed high identity to *MtNHX4*, formed a cluster of their own. The *P. vulgaris* gene, *Phvul.007G182200*, also fell in the same cluster (Fig. 3).

### Subcellular localization analyses

In general, NHX proteins are classified into three major classes, class I, class II, and class III, based on their subcellular localization to vacuole, endosomal compartments, and plasma membrane, respectively (Yokoi et al. 2002). As there is no genome-specific subcellular localization prediction software available for *M. truncatula*, we performed a bioinformatics analysis using a generalized plant localization predictor, Plant-mPLoc (Chou and Shen 2010). The localization of the class II protein to endosomal compartments was confirmed based on its transmembrane domains (Yuan and Teasdale



**Fig. 3** Phylogenetic analysis of the NHX genes in *M. truncatula*, *A. thaliana*, *Glycine max*, and *Phaseolus vulgaris*. The phylogenetic tree was constructed using MEGA 6.0 using the neighbor-joining method. Three classes of NHX genes are represented on the right side



2002). Based on the predication, MtNHX1 to MtNHX4 were localized to vacuole, MtNHX6 was localized to Golgi, and MtNHX7 was predicted to be localized to plasma membrane (Table 2). Subcellular localizations of all six *M. truncatula* proteins were in line with the localization of their corresponding AtNHX proteins (Yokoi et al. 2002).

**Expression profiles of *M. truncatula* NHX genes in different tissues**

To study the expression profiles of the MtNHX genes in different *M. truncatula* tissues, the expression levels were analyzed using qRT-PCR (Fig. 4). *MtNHX1*, *MtNHX6*, and *MtNHX7* showed the highest expression levels in leaves (Fig. 4). *MtNHX2* and *MtNHX3* had the highest expression

in flowers; expression levels in other tissues were relatively low. *MtNHX4* had the highest expression in pods. Interestingly, in comparison to the other MtNHX genes, *MtNHX2* and *MtNHX3* had really low expression levels in roots. *MtNHX1* exhibited very little variation in expression among different tissues tested (Fig. 4).

**Effect of salinity on biomass and ion composition**

Shoot and root biomasses were determined for the control and salt treatments. The average shoot biomass was 1.540 g p<sup>-1</sup> dw and 1.205 g p<sup>-1</sup> dw in the control and salt treatments, respectively; the average root biomass was 0.220 g p<sup>-1</sup> dw and 0.177 g p<sup>-1</sup> dw in the control and salt treatments, respectively. The average shoot and root biomasses were reduced by

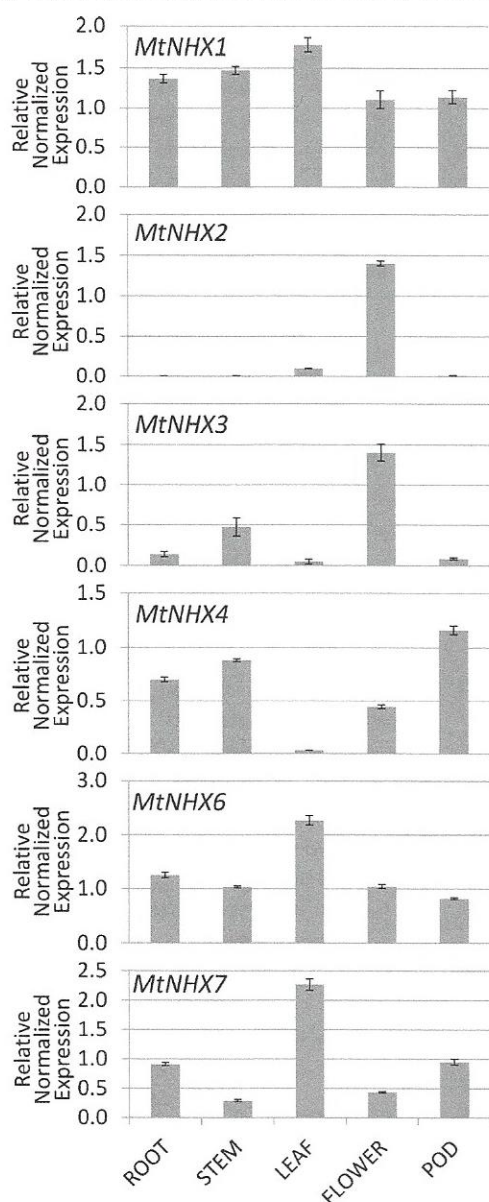


**Fig. 4** Relative gene expression of the *MtNHX* genes in different *M. truncatula* tissues. Gene expression was studied using qRT-PCR. Error bars represent standard errors of four biological replicates

21.5 and 17.4%, respectively, in the salt treatment as compared to the control.

As expected, plants accumulated higher amounts of  $\text{Na}^+$  and  $\text{Cl}^-$  in shoot and root tissues under salt treatment. There was 178 and 75% increase in  $\text{Na}^+$  accumulation in salt treatment in shoots and roots, respectively (Fig. 5). Similarly,  $\text{Cl}^-$  content increased by 152 and 162% in shoots and roots, respectively. On the other hand,  $\text{K}^+$  content decreased by 24 and 29% in salt treatment in shoots and roots, respectively (Fig. 5). The  $\text{Na}^+/\text{K}^+$  ratio in the salt treatment as compared to the control increased 3.64-fold and 2.57-fold in shoots and roots, respectively (Fig. 5).

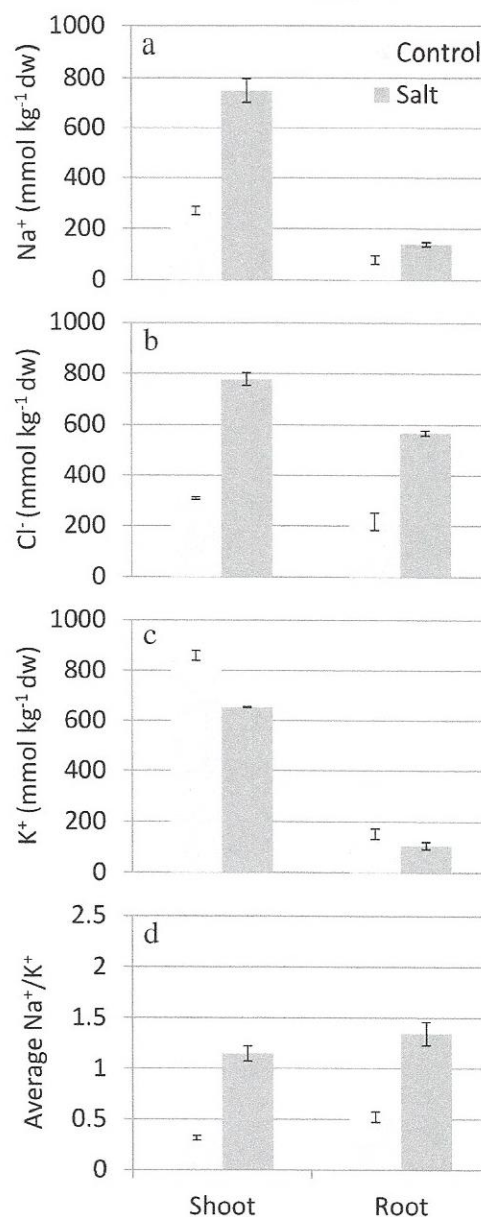


**Fig. 5** Shoot- and root-ion concentrations of *M. truncatula* plants in the control and the salt treatments. **a** Average  $\text{Na}^+$  concentration, **b** average  $\text{Cl}^-$  concentration, **c** average  $\text{K}^+$  concentration, **d** average  $\text{Na}^+/\text{K}^+$  content. Error bars represent standard errors of four biological replicates

### Expression profiles of the *M. truncatula* NHX genes under salinity stress

We studied expressions of the *MtNHX* genes in the control and salinity treatments using qRT-PCR. RNA was isolated from leaf and root tissues 48 h after the  $10 \text{ dS m}^{-1}$  salt treatment was initiated. Of the six genes, *MtNHX3*, *MtNHX6*, and *MtNHX7* displayed significant upregulation in salinity treatment in roots as compared to the control (Fig. 6). Interestingly, *MtNHX1* and *MtNHX2* were not upregulated in leaves or roots of salt-treated plants (Fig. 6). Except for *MtNHX3*, which was downregulated



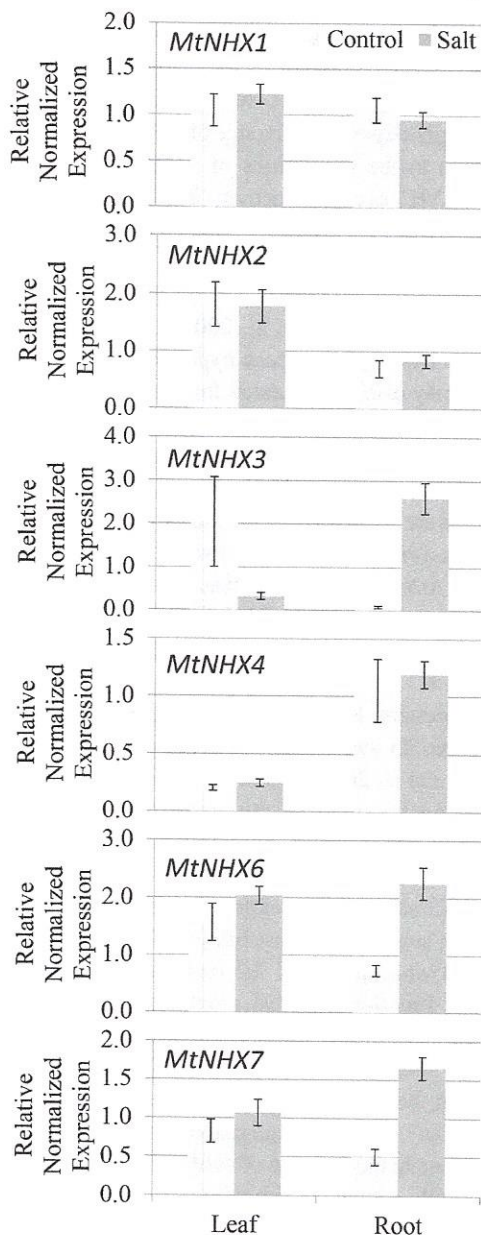


**Fig. 6** Expression of the MtNHX genes in the leaves and roots of the control and the salt treatments. Error bars represent standard errors of four biological replicates

in leaves in the salt treatment, none of the genes showed significant expression differences in leaves of the plants irrigated with the control and saline treatment (Fig. 6).

## Discussion

Salinity is one of the most important abiotic stresses, as approximately 20% of the irrigated land used for agriculture globally is affected by salt (Flowers and Yeo 1995). To deal with salt stress, plants develop physiological, biochemical,

and ecological strategies. Some common strategies include root ion uptake, root ion exclusion, ion accumulation in vacuoles of root or shoot cells, regulation of ion transport from root to shoot, increased tolerance for toxic ions, and compatible solute accumulation (Gupta and Huang 2014; Munns and Tester 2008). Although  $\text{Cl}^-$  toxicity is important in some sensitive plant species,  $\text{Na}^+$  toxicity is the primary aspect of the salinity stress (Cornacchione and Suarez 2017). Traditionally,  $\text{Na}^+$  exclusion is believed to be the primary mechanism regulating salt tolerance (Liu et al. 2015; Munns and Tester 2008). However, recent findings indicate that only a fraction of the variation in salt tolerance is explained by  $\text{Na}^+$  exclusion, suggesting roles of other component traits in the salt tolerance mechanism (Cornacchione and Suarez 2017; Genc et al. 2007; Gupta and Huang 2014; Munns and Tester 2008; Sandhu et al. 2017). It has been demonstrated that sequestration of  $\text{Na}^+$  into vacuoles is also an important strategy used by plants to keep the cytosolic concentration of  $\text{Na}^+$  low (Barragan et al. 2012; Bassil and Blumwald 2014).  $\text{Na}^+/\text{H}^+$  exchangers (NHXs) are the main players in sequestering  $\text{Na}^+$  into vacuoles and are shown to be involved in  $\text{K}^+$  homeostasis (Bassil and Blumwald 2014; Cao et al. 2016; Tian et al. 2017; Wu et al. 2017). In addition, NHX family members are involved in several cellular functions including cell expansion, stomatal regulation, pH control, vesicle trafficking, and flowering initiation (Bassil and Blumwald 2014). Understanding the way NHX family members are involved in stress regulation and homeostasis will be critical in comprehending mechanisms regulating plant growth and development. Corresponding to eight NHX genes in *Arabidopsis*, only six were identified in *M. truncatula*, of which four genes belonged to class I (vacuole specific), while one each belonged to class II (Golgi specific) and class III (plasma membrane specific). Distinction between genes within a class based on sequence homology is not very reliable due to high homology of genes even among AtNHX genes which likely arose from recent duplication events. For instance, AtNHX1 appears to be a paralog of AtNHX2, while AtNHX7 is likely a paralog of AtNHX8 (Fig. 3). Genes corresponding to *AtNHX5* and *AtNHX8* were missing in *M. truncatula*. Lack of *NHX5* in *M. truncatula* may not be critical as *NHX5* and *NHX6* were shown to be functionally redundant; as a single mutant, *nhx5* or *nhx6* did not display any obvious phenotypes (Bassil et al. 2011a). Additionally, either *NHX5* or *NHX6* was able to rescue the phenotype in the *nhx5 nhx6* double mutant (Bassil et al. 2011a). Finally, AtNHX8 is a  $\text{Li}^+/\text{H}^+$  antiporter and plays a critical role in  $\text{Li}^+$  extrusion but not for  $\text{Na}^+$  tolerance (An et al. 2007). Absence of *NHX8* in *M. truncatula* suggests differences in regulation of the  $\text{Li}^+$  detoxification mechanism in *M. truncatula* and *Arabidopsis*.

Phylogenetic analysis revealed that six MtNHX proteins fall under three subgroups. MtNHX1 through MtNHX4 are



in one subgroup, MtNHX6 is in a second subgroup, and MtNHX7 is in a third subgroup (Fig. 3). These subgroups correspond to three classes of NHXs (class I, class II, and class III). Intron-exon structures also highlighted clear differences among three classes of MtNHX genes with class I, class II, and class III genes containing 14, 21, and 3 exons, respectively (Fig. 1). There are two closely associated soybean genes corresponding to each of the *NHX1*, *NHX2*, *NHX4*, and *NHX6* genes (Fig. 3), which is expected because of the paleopolyploid nature of the soybean genome (Schmutz et al. 2010).

Structural and domain analyses revealed that 12 TM domains and an amiloride binding motif are conserved in five MtNHX proteins (Fig. 2). The amiloride binding motif is known to play an important role in inhibiting  $\text{Na}^+/\text{H}^+$  exchange on amiloride binding (Kahn 1987). However, TM5 and TM6 that are the most critical for the antiport activity (Putney et al. 2002; Yamaguchi et al. 2003) are conserved among all MtNHX proteins (Fig. 2). Based on the proposed ion transport mechanism for NHE1 in yeast, five residues (P167, P168, E262, D267, and S351) are known to play a critical role in the antiport activity (Landau et al. 2007). According to this model, P167 and P168 are predicated to lay the cation-transport path; E262 attracts  $\text{H}^+$  from the cytoplasmic side, which leads to protonation of D267, and S351 plays an important role in exchange of  $\text{H}^+$  with  $\text{Na}^+$  (Landau et al. 2007; Reddy et al. 2008). Five corresponding residues, P91, P92, E183, D188, and S274, of MtNHX1 are completely conserved in class I and class II MtNHX proteins (Fig. 2). MtNHX7/SOS1, however, is a small protein that contains only four TM domains (TM3, TM4, TM5, and TM6) (Fig. 2). Sequencing of MtNHX7/SOS1 in cultivar Jamalong A-17 confirmed that the sequencing information previously reported for MtNHX7/SOS1 ([https://phytozome.jgi.doe.gov/pz/portal.html#!info?alias=Org\\_Mtruncatula](https://phytozome.jgi.doe.gov/pz/portal.html#!info?alias=Org_Mtruncatula)) was accurate and it is a small gene (data not shown). BLAST search using the MtNHX7/SOS1 sequence did not find a homologous gene of similar size in any other plant species. Although it shows a low level of conservation with the other MtNHX proteins, E183 and D188 are conserved in MtNHX7/SOS1 (Fig. 2). AtNHX7/SOS1 is known to be a vital player that regulates  $\text{Na}^+$  efflux from roots (Shi et al. 2002). It will be interesting to investigate if the SOS pathway-based regulation of  $\text{Na}^+$  exclusion from roots is maintained in *M. truncatula*. If so, is this small MtNHX7/SOS1 sufficient to carry the function or is there an alternative mechanism to regulate  $\text{Na}^+$  efflux from roots in *M. truncatula*?

Like other NHX genes known in eukaryotes, the N-terminus of MtNHX proteins is highly conserved as compared to the C-terminus (Yamaguchi et al. 2003). Additionally, the C-termini of MtNHX6 and MtNHX7 are diverged as compared to the class I NHXs (Fig. 2). C-terminus is proposed to be involved in differential regulation of the NHX genes,

perhaps by posttranslational modifications such as phosphorylation and glycosylation or by facilitating protein-protein interactions (Yamaguchi et al. 2005; Yamaguchi et al. 2003).  $\text{Ca}^{2+}$ - and pH-dependent binding of calmodulin-like protein (AtCaM15) to the C-terminus of AtNHX1 resulted in decreased  $\text{Na}^+/\text{H}^+$  exchange activity into the vacuole as compared to the  $\text{K}^+/\text{H}^+$  exchange activity (Yamaguchi et al. 2005). During salt stress, when pH is high in the vacuole,  $\text{Na}^+/\text{H}^+$  activity is favored and more  $\text{Na}^+$  is sequestered in the vacuole (Yamaguchi et al. 2005). Although conclusive evidence is lacking, it has been hypothesized that like SOS1, AtNHX1 may also be regulated through its interaction with SOS2 (Yamaguchi et al. 2005).

As seen for NHX genes in other plants (Cao et al. 2016; Rodriguez-Rosales et al. 2009; Tian et al. 2017), different MtNHXs were expressed in all the organs tested; however, the expression levels varied for different NHX genes. Similar to *AtNHX1*, *MtNHX1* was expressed in most plant tissues (Shi and Zhu 2002). *MtNHX3* had the highest expression levels in the flowers (Fig. 4), as seen for *AtNHX3* that is critical for  $\text{K}^+$  accumulation in vacuoles (Liu et al. 2010). Lower expression levels of *MtNHX4* in leaves and flowers as compared to stems and roots are also consistent with *AtNHX4* (Li et al. 2009). There were some differences in expression patterns of *M. truncatula* as compared to *Arabidopsis*. For instance, *AtNHX2* was highly expressed in root and leaf tissues (Rodriguez-Rosales et al. 2009); however, *MtNHX2* showed low expression in these tissues. This observation suggests the possibility of functional differences between *Arabidopsis* and *M. truncatula* NHX proteins. Additional functional analyses will help in differentiating these genes and further refining the orthologous relationship between *Arabidopsis* and *M. truncatula* NHX genes.

Plants in the salinity treatment had increases of 178 and 152% for  $\text{Na}^+$  and  $\text{Cl}^-$  accumulation in shoots, respectively (Fig. 5). Despite the increase of 4666% in  $\text{Na}^+$  as compared to 2014% in  $\text{Cl}^-$  content of irrigation water in the saline treatment (Table 1), roots presented only 75% increase in  $\text{Na}^+$  accumulation as compared to 162% for  $\text{Cl}^-$  (Fig. 5). The relatively smaller increase in  $\text{Na}^+$  accumulation as compared to  $\text{Cl}^-$  in roots of salt-treated plants may be due to an effective  $\text{Na}^+$  exclusion mechanism in roots. Although the  $\text{K}^+$  content was similar in irrigation water of the control and saline treatments ( $5 \text{ mmol}_e \text{ L}^{-1}$ ), the  $\text{K}^+$  content decreased significantly in the salt treatment in shoots (24% decrease) and roots (29% decrease), as compared to that in the control. This is consistent with many other plant species and can be explained as some protein channels play an important role in transporting  $\text{Na}^+$  and  $\text{K}^+$  (Kumari et al. 2015; Ors and Suarez 2016; Sandhu et al. 2017; Semiz and Suarez 2015; Tounsi et al. 2017).

Expression analyses showed that the *MtNHX3*, *MtNHX6*, and *MtNHX7* genes were upregulated in salinity treatment in roots (Fig. 6). AtNHX3 is known to play an important role in



$K^+/H^+$  exchange and facilitates more  $K^+$  accumulation in the vacuole as compared to  $Na^+$  (Liu et al. 2010). AtNHX6 is located in TGN, Golgi, and other endosomal compartments and plays a role in the trafficking of proteins to vacuoles (Bassil et al. 2011a). NHX7/SOS1 is critical for excluding  $Na^+$  from plant roots (Shi et al. 2002). Upregulated expressions of *MtNHX3*, *MtNHX6*, and *MtNHX7* in our salinity treatment support the idea that their roles in response to salt stress may be conserved in *M. truncatula*. Surprisingly, *MtNHX1* and *MtNHX2*, homologs of which are critical players in maintaining turgor regulation via active  $K^+$  uptake at the tonoplast during salt stress in *Arabidopsis* (Barragan et al. 2012), did not show any significant change in gene expression in our salinity treatment as compared to the control (Fig. 6). These observations may suggest some functional differences in NHX proteins among different plant species. Expression analysis in leaves displayed no critical differences between the control and the salt treatment suggesting that in addition to sequestering  $Na^+$  into vacuoles, other component traits of the salt tolerance mechanism may be crucial in *M. truncatula*.

Although the biological functions of NHX family members are not studied in detail in this investigation, bioinformatics and expression analyses suggest that NHX family members in *M. truncatula* may also be involved in maintaining homeostasis in vacuoles and may be important players during salinity stress.

**Acknowledgements** Acknowledgements are due to Pangki Xiong for help in ion analyses.

## References

- An R, Chen QJ, Chai MF, Lu PL, Su Z, Qin ZX, Chen J, Wang XC (2007) *AtNHX8*, a member of the monovalent cation: proton antiporter-1 family in *Arabidopsis thaliana*, encodes a putative  $Li^+/H^+$  antiporter. *Plant J* 49(4):718–728. <https://doi.org/10.1111/j.1365-313X.2006.02990.x>
- Apse MP, Aharon GS, Snedden WA, Blumwald E (1999) Salt tolerance conferred by overexpression of a vacuolar  $Na^+/H^+$  antiporter in *Arabidopsis*. *Science* 285(5431):1256–1258. <https://doi.org/10.1126/science.285.5431.1256>
- Barragan V, Leidi EO, Andres Z, Rubio L, De Luca A, Fernandez JA, Cubero B, Pardo JM (2012) Ion exchangers NHX1 and NHX2 mediate active potassium uptake into vacuoles to regulate cell turgor and stomatal function in *Arabidopsis*. *Plant Cell* 24(3):1127–1142. <https://doi.org/10.1105/tpc.111.095273>
- Bassil E, Blumwald E (2014) The ins and outs of intracellular ion homeostasis: NHX-type cation/ $H^+$  transporters. *Curr Opin Plant Biol* 22:1–6. <https://doi.org/10.1016/j.pbi.2014.08.002>
- Bassil E, Ohto MA, Esumi T, Tajima H, Zhu Z, Cagnac O, Belmonte M, Peleg Z, Yamaguchi T, Blumwald E (2011a) The *Arabidopsis* intracellular  $Na^+/H^+$  antiporters NHX5 and NHX6 are endosome associated and necessary for plant growth and development. *Plant Cell* 23(1):224–239. <https://doi.org/10.1105/tpc.110.079426>
- Bassil E, Tajima H, Liang YC, Ohto MA, Ushijima K, Nakano R, Esumi T, Coku A, Belmonte M, Blumwald E (2011b) The *Arabidopsis*  $Na^+/H^+$  antiporters NHX1 and NHX2 control vacuolar pH and  $K^+$  homeostasis to regulate growth, flower development, and reproduction. *Plant Cell* 23(9):3482–3497. <https://doi.org/10.1105/tpc.111.089581>
- Cao B, Long D, Zhang M, Liu C, Xiang Z, Zhao A (2016) Molecular characterization and expression analysis of the mulberry  $Na^+/H^+$  exchanger gene family. *Plant Physiol Biochem* 99:49–58. <https://doi.org/10.1016/j.plaphy.2015.12.010>
- Chou K-C, Shen H-B (2010) Plant-mPLoc: a top-down strategy to augment the power for predicting plant protein subcellular localization. *PLoS One* 5(6):e11335. <https://doi.org/10.1371/journal.pone.0011335>
- Cooley H, Donnelly K, Phurisamban R, Subramanian M (2015) Impacts of California's ongoing drought: agriculture. Pacific Institute, Oakland
- Cornacchione MV, Suarez DL (2017) Evaluation of alfalfa (*Medicago sativa* L.) populations' response to salinity stress. *Crop Sci* 57(1):137–150. <https://doi.org/10.2135/cropsci2016.05.0371>
- Counillon L, Franchi A, Pouyssegur J (1993) A point mutation of the  $Na^+/H^+$  exchanger gene (*NHE1*) and amplification of the mutated allele confer amiloride resistance upon chronic acidosis. *Proc Natl Acad Sci U S A* 90(10):4508–4512. <https://doi.org/10.1073/pnas.90.10.4508>
- Edgar RC (2004) MUSCLE: multiple sequence alignment with high accuracy and high throughput. *Nucleic Acids Res* 32(5):1792–1797. <https://doi.org/10.1093/nar/gkh340>
- Flowers TJ, Yeo AR (1995) Breeding for salinity resistance in crop plants: where next? *Aust J Plant Physiol* 22(6):875–884. <https://doi.org/10.1071/PP9950875>
- Genç Y, McDonald GK, Tester M (2007) Reassessment of tissue  $Na^+$  concentration as a criterion for salinity tolerance in bread wheat. *Plant Cell Environ* 30(11):1486–1498. <https://doi.org/10.1111/j.1365-3040.2007.01726.x>
- Graham PH, Vance CP (2003) Legumes: importance and constraints to greater use. *Plant Physiol* 131(3):872–877. <https://doi.org/10.1104/pp.017004>
- Gupta B, Huang BR (2014) Mechanism of salinity tolerance in plants: physiological, biochemical, and molecular characterization. *Int J Genomics* 2014, Article ID 701596:18 pages. <https://doi.org/10.1155/2014/701596>
- Hu B, Jin J, Guo A-Y, Zhang H, Luo J, Gao G (2015) GSDB 2.0: an upgraded gene feature visualization server. *Bioinformatics* 31(8):1296–1297. <https://doi.org/10.1093/bioinformatics/btu817>
- Jiang X, Leidi EO, Pardo JM (2010) How do vacuolar NHX exchangers function in plant salt tolerance? *Plant Signal Behav* 5(7):792–795. <https://doi.org/10.4161/psb.5.7.11767>
- Kahn AM (1987) Difference between human red blood cell  $Na^+-Li^+$  countertransport and renal  $Na^+-H^+$  exchange. *Hypertension* 9(1):7–12. <https://doi.org/10.1161/01.HYP.9.1.7>
- Krogh A, Larsson B, von Heijne G, Sonnhammer EL (2001) Predicting transmembrane protein topology with a hidden Markov model: application to complete genomes. *J Mol Biol* 305(3):567–580. <https://doi.org/10.1006/jmbi.2000.4315>
- Kumari S, Joshi R, Singh K, Roy S, Tripathi AK, Singh P, Singla-Pareek SL, Pareek A (2015) Expression of a cyclophilin OsCyp2-P isolated from a salt-tolerant landrace of rice in tobacco alleviates stress via ion homeostasis and limiting ROS accumulation. *Funct Integr Genomics* 15(4):395–412. <https://doi.org/10.1007/s10142-014-0429-5>
- Landau M, Herz K, Padan E, Ben-Tal N (2007) Model structure of the  $Na^+/H^+$  exchanger 1 (NHE1): functional and clinical implications. *J Biol Chem* 282(52):37854–37863. <https://doi.org/10.1074/jbc.M705460200>
- Li HT, Liu H, Gao XS, Zhang H (2009) Knock-out of *Arabidopsis AtNHX4* gene enhances tolerance to salt stress. *Biochem Biophys Res Commun* 382(3):637–641. <https://doi.org/10.1016/j.bbrc.2009.03.091>



- Liu L (1998) Determination of chloride in plant tissue. In: Kalra YP (ed) Handbook of reference methods of plant analysis. CRC Press, Boca Raton, pp 111–113
- Liu H, Tang R, Zhang Y, Wang C, Lv Q, Gao X, Li W, Zhang H (2010) AtNHX3 is a vacuolar  $K^+/H^+$  antiporter required for low-potassium tolerance in *Arabidopsis thaliana*. Plant Cell Environ 33(11):1989–1999. <https://doi.org/10.1111/j.1365-3040.2010.02200.x>
- Liu M, Wang T-Z, Zhang W-H (2015) Sodium extrusion associated with enhanced expression of SOS1 underlies different salt tolerance between *Medicago falcata* and *Medicago truncatula* seedlings. Environ Exp Bot 110:46–55. <https://doi.org/10.1016/j.envexpbot.2014.09.005>
- Mishra S, Alavilli H, Lee BH, Panda SK, Sahoo L (2014) Cloning and functional characterization of a vacuolar  $Na^+/H^+$  antiporter gene from mungbean (*VrNHX1*) and its ectopic expression enhanced salt tolerance in *Arabidopsis thaliana*. PLoS One 9(10):e106678. <https://doi.org/10.1371/journal.pone.0106678>
- Munns R, Tester M (2008) Mechanisms of salinity tolerance. Annu Rev Plant Biol 59(1):651–681. <https://doi.org/10.1146/annurev.arplant.59.032607.092911>
- Ors S, Suarez DL (2016) Salt tolerance of spinach as related to seasonal climate. Hort Sci (Prague) 43(1):33–41. <https://doi.org/10.17221/114/2015-HORTSCI>
- Pardo JM, Cubero B, Leidi EO, Quintero FJ (2006) Alkali cation exchangers: roles in cellular homeostasis and stress tolerance. J Exp Bot 57(5):1181–1199. <https://doi.org/10.1093/jxb/erj114>
- Putney LK, Denker SP, Barber DL (2002) The changing face of the  $Na^+/H^+$  exchanger, NHE1: structure, regulation, and cellular actions. Annu Rev Pharmacol Toxicol 42(1):527–552. <https://doi.org/10.1146/annurev.pharmtox.42.092001.143801>
- Qiu Q-S, Guo Y, Dietrich MA, Schumaker KS, Zhu J-K (2002) Regulation of SOS1, a plasma membrane  $Na^+/H^+$  exchanger in *Arabidopsis thaliana*, by SOS2 and SOS3. Proc Natl Acad Sci U S A 99(12):8436–8441. <https://doi.org/10.1073/pnas.122224699>
- Rajagopal D, Agarwal P, Tyagi W, Singla-Pareek SL, Reddy MK, Sopory SK (2007) *Pennisetum glaucum*  $Na^+/H^+$  antiporter confers high level of salinity tolerance in transgenic *Brassica juncea*. Mol Breed 19(2):137–151. <https://doi.org/10.1007/s11032-006-9052-z>
- Reddy T, Ding J, Li X, Sykes BD, Rainey JK, Fliegel L (2008) Structural and functional characterization of transmembrane segment IX of the NHE1 isoform of the  $Na^+/H^+$  exchanger. J Biol Chem 283(32):22018–22030. <https://doi.org/10.1074/jbc.M803447200>
- Rodríguez-Rosales MP, Jiang X, Galvez FJ, Aranda MN, Cubero B, Venema K (2008) Overexpression of the tomato  $K^+/H^+$  antiporter LeNHX2 confers salt tolerance by improving potassium compartmentalization. New Phytol 179(2):366–377. <https://doi.org/10.1111/j.1469-8137.2008.02461.x>
- Rodríguez-Rosales MP, Galvez FJ, Huertas R, Aranda MN, Baghour M, Cagnac O, Venema K (2009) Plant NHX cation/proton antiporters. Plant Signal Behav 4(4):265–276. <https://doi.org/10.4161/psb.4.4.7919>
- Saitou N, Nei M (1987) The neighbor-joining method: a new method for reconstructing phylogenetic trees. Mol Biol Evol 4:406–425. <https://doi.org/10.1093/oxfordjournals.molbev.a040454>
- Sandhu D, Cornacchione MV, Ferreira JFS, Suarez DL (2017) Variable salinity responses of 12 alfalfa genotypes and comparative expression analyses of salt-response genes. Sci Rep 7:42958. <https://doi.org/10.1038/srep42958>
- Schmutz J, Cannon SB, Schlueter S, Ma J, Mitros T, Nelson W, Hyten DL, Song Q, Thelen JJ, Cheng J, Xu D, Hellsten U, May GD, Yu Y, Sakurai T, Umezawa T, Battacharyya MK, Sandhu D, Valliyodan B, Lindquist E, Peto M, Grant D, Shu S, Goodstein D, Barry K, Futrell-Griggs M, Abernathy B, Du J, Tian Z, Zhu L, Gill N, Joshi T, Libault M, Sethuraman A, Zhang X-C, Shinozaki K, Nguyen HT, Wing RA, Cregan P, Specht J, Grimwood J, Rokhsar D, Stacey G, Shoemaker RC, Jackson SA (2010) Genome sequence of the palaeopolyploid soybean. Nature 463(7278):178–183. <https://doi.org/10.1038/nature08670>
- Semiz GD, Suarez DL (2015) Tomato salt tolerance: impact of grafting and water composition on yield and ion relations. Turk J Agric For 39:876–886. <https://doi.org/10.3906/tar-1412-106>
- Shavrukov Y (2013) Salt stress or salt shock: which genes are we studying? J Exp Bot 64(1):119–127. <https://doi.org/10.1093/jxb/ers316>
- Shi H, Zhu JK (2002) Regulation of expression of the vacuolar  $Na^+/H^+$  antiporter gene *AtNHX1* by salt stress and abscisic acid. Plant Mol Biol 50(3):543–550. <https://doi.org/10.1023/A:1019859319617>
- Shi H, Quintero FJ, Pardo JM, Zhu J-K (2002) The putative plasma membrane  $Na^+/H^+$  antiporter SOS1 controls long-distance  $Na^+$  transport in plants. Plant Cell 14(2):465–477. <https://doi.org/10.1105/tpc.010371>
- Sievers F, Wilm A, Dineen D, Gibson TJ, Karplus K, Li W, Lopez R, McWilliam H, Remmert M, Söding J, Thompson JD, Higgins DG (2011) Fast, scalable generation of high-quality protein multiple sequence alignments using Clustal Omega. Mol Syst Biol 7(1):539. <https://doi.org/10.1038/msb.2011.75>
- Sze H, Padmanaban S, Cellier F, Honys D, Cheng NH, Bock KW, Conejero G, Li X, Twell D, Ward JM, Hirschi KD (2004) Expression patterns of a novel *AtCHX* gene family highlight potential roles in osmotic adjustment and  $K^+$  homeostasis in pollen development. Plant Physiol 136(1):2532–2547. <https://doi.org/10.1104/pp.104.046003>
- Tamura K, Stecher G, Peterson D, Filipski A, Kumar S (2013) MEGA6: Molecular Evolutionary Genetics Analysis version 6.0. Mol Biol Evol 30(12):2725–2729. <https://doi.org/10.1093/molbev/mst197>
- Tang H, Krishnakumar V, Bidwell S, Rosen B, Chan A, Zhou S, Gentzmittel L, Childs KL, Yandell M, Gundlach H, Mayer KF, Schwartz DC, Town CD (2014) An improved genome release (version Mt4.0) for the model legume *Medicago truncatula*. BMC Genomics 15(1):312. <https://doi.org/10.1186/1471-2164-15-312>
- Tester M, Davenport R (2003)  $Na^+$  tolerance and  $Na^+$  transport in higher plants. Ann Bot 91(5):503–527. <https://doi.org/10.1093/aob/mcg058>
- Tian F, Chang E, Li Y, Sun P, Hu J, Zhang J (2017) Expression and integrated network analyses revealed functional divergence of NHX-type  $Na^+/H^+$  exchanger genes in poplar. Sci Rep 7(1):2607. <https://doi.org/10.1038/s41598-017-02894-8>
- Tounsi S, Feki K, Hmidi D, Masmoudi K, Brini F (2017) Salt stress reveals differential physiological, biochemical and molecular responses in *T. monococcum* and *T. durum* wheat genotypes. Physiol Mol Biol Plants 23(3):517–528. <https://doi.org/10.1007/s12298-017-0457-4>
- Vandesompele J, De Preter K, Pattyn F, Poppe B, Van Roy N, De Paep A, Speleman F (2002) Accurate normalization of real-time quantitative RT-PCR data by geometric averaging of multiple internal control genes. Genome Biol 3:research0034 0031-research0034.0011
- Wu Y, Meng K, Liang X (2017) Distinct patterns of natural selection in  $Na^+/H^+$  antiporter genes in *Populus euphratica* and *Populus pruinosa*. Ecol Evol 7(1):82–91. <https://doi.org/10.1002/ece3.2639>
- Xue Z-Y, Zhi D-Y, Xue G-P, Zhang H, Zhao Y-X, Xia G-M (2004) Enhanced salt tolerance of transgenic wheat (*Triticum aestivum* L.) expressing a vacuolar  $Na^+/H^+$  antiporter gene with improved grain yields in saline soils in the field and a reduced level of leaf  $Na^+$ . Plant Sci 167(4):849–859. <https://doi.org/10.1016/j.plantsci.2004.05.034>
- Yamaguchi T, Apse MP, Shi H, Blumwald E (2003) Topological analysis of a plant vacuolar  $Na^+/H^+$  antiporter reveals a luminal C terminus that regulates antiporter cation selectivity. Proc Natl Acad Sci U S A 100(21):12510–12515. <https://doi.org/10.1073/pnas.2034966100>
- Yamaguchi T, Aharon GS, Sotosanto JB, Blumwald E (2005) Vacuolar  $Na^+/H^+$  antiporter cation selectivity is regulated by calmodulin from within the vacuole in a  $Ca^{2+}$ - and pH-dependent manner. Proc Natl



- Acad Sci U S A 102(44):16107–16112. <https://doi.org/10.1073/pnas.0504437102>
- Yokoi S, Quintero FJ, Cubero B, Ruiz MT, Bressan RA, Hasegawa PM, Pardo JM (2002) Differential expression and function of *Arabidopsis thaliana* NHX Na<sup>+</sup>/H<sup>+</sup> antiporters in the salt stress response. *Plant J* 30(5):529–539. <https://doi.org/10.1046/j.1365-313X.2002.01309.x>
- Yuan Z, Teasdale RD (2002) Prediction of Golgi type II membrane proteins based on their transmembrane domains. *Bioinformatics* 18(8): 1109–1115. <https://doi.org/10.1093/bioinformatics/18.8.1109>
- Zhang HX, Blumwald E (2001) Transgenic salt-tolerant tomato plants accumulate salt in foliage but not in fruit. *Nat Biotechnol* 19(8): 765–768. <https://doi.org/10.1038/90824>
- Zhang YM, Zhang HM, Liu ZH, Li HC, Guo XL, Li GL (2015) The wheat NHX antiporter gene *TaNHX2* confers salt tolerance in transgenic alfalfa by increasing the retention capacity of intracellular potassium. *Plant Mol Biol* 87(3):317–327. <https://doi.org/10.1007/s11103-014-0278-6>
- Zuckerkindl E, Pauling L (1965) Evolutionary divergence and convergence in proteins. In: Bryson V, Vogel HJ (eds) *Evolving Genes and Proteins*. Academic Press, New York, pp 97–166. <https://doi.org/10.1016/B978-1-4832-2734-4.50017-6>

Mention of trade names or commercial products in this publication is solely for the purpose of providing specific information and does not imply recommendation or endorsement by the U.S. Department of Agriculture.



